Modelling seismic waves propagating within the Earth

Abstract

In this essay we look at a 2-dimensional seismic wave model to simulate a brief excitation and predict the resulting wave propagation. We will use numerical methods to discretise and solve of the wave equation. The model measures the perceived signal at three different detectors and utilizes a simple ray model to identify distinct waves. This allows for improved interpretation of the results since the distinct waves have a known signal.

1 Introduction

A seismic wave is a wave of acoustic energy that travels through the Earth[1], the most common ones are the ones generated by earthquakes. Geologists utilize artificial seismic waves to infer the underlying structure of the Earth, while controlling for external variables. This method can be utilized to understand the composition of different layers and map subsurface structures, such as caves. The insights gained from this work have numerous applications, including aiding in landslide rescue operations and natural resource exploration. It would be extremely useful to have a model that can replicate the results of the artificial wave generation process without the need for physical experimentation. Such a model would enable quick and inexpensive testing of various theories, including how waves respond to changes in amplitude, frequency, and medium. Additionally, this model could be used to calibrate detector receivers and optimize their positioning before costly real-world tests are conducted. In order to derive our model we must firstly look at the assumptions we have made in order to simplify the problem.

2 Coordiante System

The Earth is primarily composed of even 3D layers of homogeneous rock. In our model, we will simplify this structure by implementing a 2D 3-layer model in which each layer has its own properties. We will enforce absorbing boundaries on the sides and bottom to ensure that our model is well-defined. When a wave hits a boundary between two layers, it will be partially reflected and partially refracted. Waves can travel in two different forms, P-waves and S-waves, which each travel at different speeds and are affected by the density of the medium they travel through. Our coordinate system will be a cross section of the Earth defined as a 2D grid with x along the horizontal and z along the vertical as seen below.

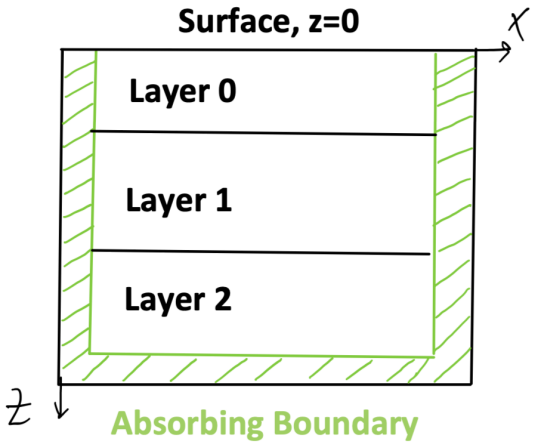

Figure 1: Layer Structure and the Damping Region.

Later we will define in greater detail the properties of these layers and observe how our waves will propagate differently through them. Next we will look at the wave equation which can be used to describe how waves generated propagate through the domain described above.

3 The Wave Equation

The Wave equation describes vibrations in a solid considering the initial displacement of each point with respect to its rest position U_i. In general this is a 3 component vector given by [2].

$$\begin{aligned} \rho\frac{\partial^2 u_i}{\partial t^2} &= (\lambda+\mu)\sum_{j=1}^{3}\frac{\partial^2 u_j}{\partial x_i \partial x_j} + \mu\sum_{j=1}^{3}\frac{\partial^2 u_i}{\partial x_j \partial x_j}, \\ &= (\lambda+\mu)[\frac{\partial^2 u_1}{\partial x_i \partial x_1} + \frac{\partial^2 u_2}{\partial x_i \partial x_2} + \frac{\partial^2 u_3}{\partial x_i \partial x_3}], \\ &+ \mu(\frac{\partial^2 u_i}{\partial x_1^2} + \frac{\partial^2 u_i}{\partial x_2^2} + \frac{\partial^2 u_i}{\partial x_3^2}), \end{aligned} \tag{1}$$

where λ and μ are rock properties called lamé parameters and ρ describes the rock density. However, using our assumptions we can simplify this equation from 3D to 2D. We shall do this by setting $u_2 = 0$ and $\frac{\partial u_i}{\partial x_2} = 0$, resulting in particles only vibrating in our cross section of the Earth. In addition, we will set $x = x_1$ and $z = x_3$ Applying this to equation (1) we get the following 2 equations:

$$\rho\frac{\partial^2 v}{\partial t^2} = (\lambda+\mu)(\frac{\partial^2 v}{\partial x^2} + \frac{\partial^2 w}{\partial x \partial z}) + \mu(\frac{\partial^2 v}{\partial x^2} + \frac{\partial^2 v}{\partial z^2}), \tag{2}$$

$$\rho\frac{\partial^2 w}{\partial t^2} = (\lambda+\mu)(\frac{\partial^2 w}{\partial z^2} + \frac{\partial^2 v}{\partial x \partial z}) + \mu(\frac{\partial^2 w}{\partial x^2} + \frac{\partial^2 w}{\partial z^2}). \tag{3}$$

Since we are looking at the Earth through a cross section our parameters ρ, λ and μ will only be a function of depth z not horizontal position x since we will assume each layer has a constant thickness. Later we will solve equations (2) and (3) numerically but first we will look for analytic solutions.

4 Analytic solutions of the Wave eqaution

Due to complexity of our wave equations our best approach to finding an analytic solution is to have a best guess and then verify our guess. Initially to simplify our equation we can define $w = 0$ and assume λ, μ and ρ to be constant. We know that any solution must be an oscillating function with respect to both time and horizontal displacement, so a general form incorporating this would be:

$$v(x,t) = A_P \sin(k_P x - \omega_P t), \qquad w = 0, \tag{4}$$

where A_P, k_P and ω_P are constants. Substituting (4) and $w = 0$ into (2): Q1

$$\rho v(x,t)(-\omega_P^2) = v(x,t)(\lambda+\mu)(-k_p^2) - v(x,t)(\mu k_P^2), \tag{5}$$

$$\rho\frac{\omega_P^2}{k_P^2} = \lambda + 2\mu,$$

$$V_P = \frac{\omega_P}{k_P} = \sqrt{\frac{\lambda+2\mu}{\rho}}. \tag{6}$$

It can also be shown that (4) is a solution to (3):

$$\begin{aligned} \rho(0) &= (\lambda+\mu)(0) + \mu(0), \\ 0 &= 0. \end{aligned}$$

Another possible analytic solution of (2) and (3) is whereby the horizontal displacement v is dependent on its vertical position as well as the time. A general solution to this would be:

$$v(z,t) = A_S \sin(k_S z - \omega_S t). \tag{7}$$

We can show that (7) is also a solution of both (2) and (3), substituting into (2):

$$\begin{aligned} \rho v(z,t)(-\omega_S^2) &= v(z,t)(\lambda+\mu)(0) + v(z,t)(\mu)(0-k_S^2), \\ V_s &= \frac{\omega_S}{k_S} = \sqrt{\frac{\mu}{\rho}}, \end{aligned} \tag{8}$$

substituting into (3):

$$\begin{aligned} \rho(0) &= (\lambda+\mu)(0) + \mu(0), \\ 0 &= 0. \end{aligned} \tag{9}$$

There are 2 types of waves: P waves (also referred to as primary or pressure waves) and S waves (secondary or shear waves). These two types of waves travel at different speed: V_p expressed by (6) and V_S expressed by (8) respectively and they depend on the density and the mechanical properties of the rocks. Note that the small displacements making a P wave are parallel to the travelling direction of the wave while for S waves, they are perpendicular to it. The equations (6) and (8) can be interpreted as the speed of the corresponding waves since the peak of the Sine wave must remain at a constant relative displacement as time increases. This means the phase difference of the Sine wave must also remain constant, ie,

$$\begin{aligned} k_P x - \omega_P t &= c, \\ \omega_P t &= k_P x - c, \\ \frac{\omega_P t}{k_P} &= x - \frac{c}{k_p}, \\ \frac{\omega_P \Delta t}{k_P} &= \Delta x, \\ \frac{\Delta x}{\Delta t} &= \frac{\omega_P}{k_P}, \\ V_P &= \frac{\omega_P}{k_P}. \end{aligned}$$

The same methodology can be used to show that V_S is the speed for S waves.

We have now shown that v as a function of either z or x and t is a solution to the wave equations (2) and (3). We can now propose a general solution that combines both approaches: **Q2**

$$f(x,z,t) = A \sin(k(\alpha x + \beta z) - \omega t). \tag{10}$$

Instead of setting $w = 0$ as done previously we can have both v and w be linear combinations of this general solution:

$$v = \alpha f(x,z,t), \tag{11}$$

$$w = \beta f(x,z,t). \tag{12}$$

In order to keep the equations normalised we can define that $\alpha^2 + \beta^2 = 1$. Again we can show that together (11) and (12) are a solution to both (2) and (3). We again verify this by substituting v and w into (2) and then use the relation, $w = \frac{\beta v}{\alpha}$:

$$\begin{aligned}\rho v(x,z,t)(-\omega^2) &= (\lambda+\mu)[-k^2\alpha^2 v(x,z,t) - k^2\alpha\beta w(x,z,t)],\\ &+ \mu(-k^2\alpha^2 v(x,z,t) - k^2\beta^2 w(x,z,t)),\\ &= -k^2 v(\lambda+\mu)(\alpha^2+\beta^2) - \mu k^2 v(\alpha^2+\beta^2),\\ V_P &= \frac{\omega}{k} = \sqrt{\frac{\lambda+2\mu}{\rho}}. \end{aligned} \tag{13}$$

The same can be done for (3), however this time using the rearrangement of the relation, $v = \frac{\alpha w}{\beta}$:

$$\begin{aligned}\rho w(x,z,t)(-\omega^2) &= (\lambda+\mu)(-k^2\alpha\beta v(x,z,t) - k^2\beta^2 w(x,z,t)\\ &+ \mu(-k^2\alpha^2 w(x,z,t) - k^2\beta w(x,z,t)),\\ &= -k^2 w(\lambda+\mu)(\alpha^2+\beta^2) - k^2\mu w(\alpha^2+\beta^2),\\ V_P &= \frac{\omega}{k} = \sqrt{\frac{\lambda+2\mu}{\rho}}. \end{aligned} \tag{14}$$

Equations (6), (13) and (14) all have the same format and describe P waves with V_P describing the speeds of the wave. Whereas, (8) refers to an S wave. We can produce other S waves by adjusting our relation between v and w. Instead by using $v = -\frac{\beta w}{\alpha}$ we can prove (2):

$$\begin{aligned}-\omega^2\rho v(x,z,t) &= (\lambda+\mu)(-k^2\alpha^2 v(x,z,t) - k^2\alpha\beta w(x,z,t))\\ &+ \mu(-k^2\alpha^2 v(x,z,t) - k^2\beta^2 v(x,z,t)),\\ &= -k^2 v(\lambda+\mu)(\alpha^2-\alpha^2) - k^2\mu v(\alpha^2+\beta^2),\\ V_S &= \frac{\omega}{k} = \sqrt{\frac{\mu}{\rho}}. \end{aligned} \tag{15}$$

We repeat using the rearrangement, $v = \frac{-\beta w}{\alpha}$:

$$\begin{aligned}-\omega^2\rho w(x,z,t) &= -k^2 w(x,z,t)(\lambda+\mu)(-\beta^2+\beta^2),\\ &- k^2\mu w(x,z,t)(\alpha^2+\beta^2),\\ V_S &= \frac{\omega}{k} = \sqrt{\frac{\mu}{\rho}}. \end{aligned} \tag{16}$$

It can be seen that by swapping β for α and multiplying by -1 we can produce S waves instead of P waves. The propagation of the wave is in the direction $\begin{pmatrix}\alpha\\ \beta\end{pmatrix}$, since as time increases $k(\alpha x+\beta z)$ must also increase to keep the term inside sine constant. This condition is needed to ensure the peak remains at the same respective point as time increases. As $\alpha^2+\beta^2 = 1$, our vector is a unit vector and describes the waves propagation as components of x and z respectively. Another approach instead of looking for specific analytic equations that satisfy the wave equation is to descretise and solve it numerically.

5 Numerical Solutions

Here we will mimic what geologists do: generate a brief perturbation at the surface ($z = 0$) of the Earth. This will generate almost concentric waves which will propagate our rock mediums. In order to solve (2) and (3) numerically we must first discretise the equations. For our analytic solutions above we could consider an infinite domain, however, to accommodate for our numerical approach we must now impose a finite domain as follows:

$$\begin{aligned} x &\in [0, X_{\max}],\\ z &\in [0, Z_{max}], \end{aligned}$$

where $X_{max} = 4000$m and $Z_{max} = 2000$m.
In order to simulate a brief excitation we must generate an artificial seismic wave. Geologists do this using vibroseis trucks as described in the video [3]. Using our new domain we can set displacement at at the point $x = X_{max}/2$, $z = 0$, ie the center of the surface to be:

$$w(t, \frac{X_{max}}{2}, 0) = \sin(2\pi tv)exp(-tv), \quad t \in [0, \frac{1}{v}]. \tag{17}$$

4

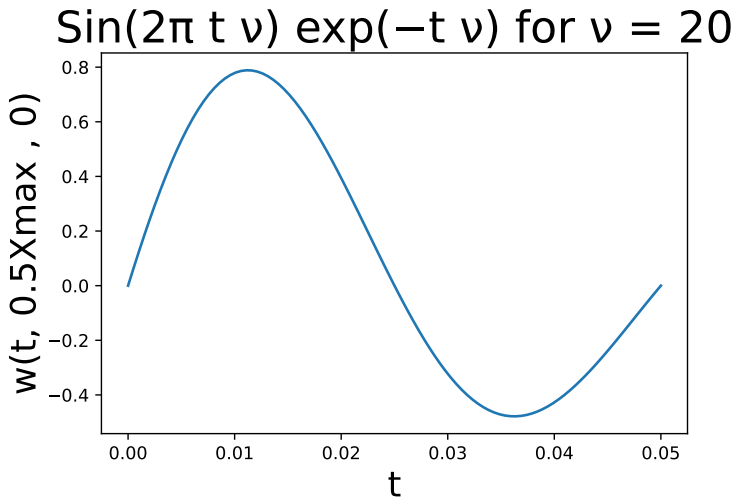

Figure 2: Initial Excitation Wave

Our next step in solving (2) and (3) numerically is to convert this system of second order differential equations in time into 2 pairs of first order differential equations in time. We can do this by setting the time derivatives of v and w to v' and w' respectively then making a substitution into (2) and (3):

$$v' = \frac{\partial v}{\partial t}, \tag{18}$$

$$w' = \frac{\partial w}{\partial t}, \tag{19}$$

$$\frac{\partial v'}{\partial t} = \frac{1}{\rho}[(\lambda+\mu)(\frac{\partial^2 v}{\partial x^2} + \frac{\partial^2 w}{\partial x \partial z}) + \mu(\frac{\partial^2 v}{\partial x^2} + \frac{\partial^2 v}{\partial z^2})], \tag{20}$$

$$\frac{\partial w'}{\partial t} = \frac{1}{\rho}[(\lambda+\mu)(\frac{\partial^2 w}{\partial z^2} + \frac{\partial^2 v}{\partial x \partial z}) + \mu(\frac{\partial^2 w}{\partial x^2} + \frac{\partial^2 w}{\partial z^2})]. \tag{21}$$

3 We can now set up a 2D lattice structure to map our functions to, our notation will be as follows:

$$f(x_i, z_j) = f_{i,j}, \tag{22}$$

$$\text{where} \quad x_i = x_0 + i\text{dx},$$

$$z_j = z_0 + j\text{dz}, \tag{23}$$

with x_0 and z_0 specifying the origin of the coordinate system. We can now show that $x_{i+1} - x_i = \text{dx}$ and $z_{j+1} - z_j = \text{dz}$. The number of lattice points in each direction will be $N_x = 1 + X_{max}/\text{dx}$ and $N_z = 1 + Z_{max}/\text{dz}$. (In what follows x_0 and z_0 will be set to 0).

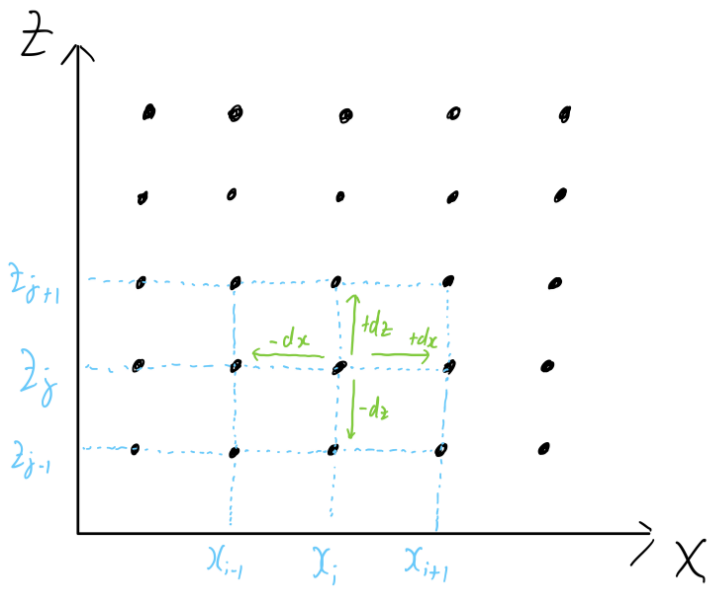

Figure 3: Lattice Structure

Now with our lattice structure we can make approximations to our partial derivatives using the Taylor series expansion in various different ways: Forward Finite Differnce, Symmetric Finite Difference and the Second Order Derivatives. We will use the following form of the general 1D Taylor series:

$$f(x) = f(x_0) + (x - x_0)\frac{\partial f(x_0)}{\partial x} + \frac{(x - x_0)^2}{2!}\frac{\partial f(x_0)}{\partial x} + o((x - x_0)^3). \tag{24}$$

5.1 Forward Finite Difference

When approximating $\frac{\partial f}{\partial x}(x_i, j_z)$ we can hold the z_j component constant as the partial derivative is only in terms of x. For this approximation we can look a finite dx increase from x_i The Taylor series of expansion of $f(x_{i+1}, z_j)$:

$$\begin{aligned} f_{i+1,j} &= f_{i,j} + \mathrm{dx}\frac{\partial f}{\partial x}(x_i, z_j) + o(\mathrm{dx}^2), \\ \frac{\partial f}{\partial x}(x_i, z_j) &= \frac{f_{i+1,j} - f_{i,j}}{\mathrm{dx}} + o(\mathrm{dx}). \end{aligned} \tag{25}$$

5.2 Symmetric Finite Difference

For this approximation we can look at a finite difference dx each way from x_i:

$$\begin{aligned} f_{i+1,j} &= f_{i,j} + \mathrm{dx}\frac{\partial f}{\partial x}(x_i, z_j) + \frac{\mathrm{dx}^2}{2}\frac{\partial^2 f}{\partial x^2}(x_i, z_j), \\ &+ \frac{\mathrm{dx}^3}{6}\frac{\partial^3 f}{\partial x^3}(x_i, z_j) + \frac{\mathrm{dx}^4}{24}\frac{\partial^4 f}{\partial x^4}(x_i, z_j) + o(\mathrm{dx}^5), \end{aligned} \tag{26}$$

$$\begin{aligned} f_{i-1,j} &= f_{i,j} - \mathrm{dx}\frac{\partial f}{\partial x}(x_i, z_j) + \frac{\mathrm{dx}^2}{2}\frac{\partial^2 f}{\partial x^2}(x_i, z_j), \\ &- \frac{\mathrm{dx}^3}{6}\frac{\partial^3 f}{\partial x^3}(x_i, z_j) + \frac{\mathrm{dx}^4}{24}\frac{\partial^4 f}{\partial x^4}(x_i, z_j) + o(\mathrm{dx}^5). \end{aligned} \tag{27}$$

We can now perform the operation (26) - (27),

$$\begin{aligned} f_{i+1,j} - f_{i-1,j} &= 2\mathrm{dx}\frac{\partial f}{\partial x}(x_i, z_j) + o(\mathrm{dx}^3), \\ \frac{\partial f}{\partial x}(x_i, z_j) &= \frac{f_{i+1,j} - f_{i-1,j}}{2\mathrm{dx}} + o(\mathrm{dx}^2). \end{aligned} \tag{28}$$

5.3 Second Order Derivatives

We can employ the same process used previously but perform (26) + (27),

$$\begin{aligned} f_{i+1,j} + f_{i-1,j} &= 2f_{i,j} + \mathrm{dx}^2\frac{\partial^2 f}{\partial x^2}(x_i, z_j) + o(\mathrm{dx}^4), \\ \frac{\partial^2 f}{\partial x^2}(x_i, z_j) &= \frac{f_{i+1,j} + f_{i-1,j} - 2f_{i,j}}{\mathrm{dx}^2} + o(\mathrm{dx}^2). \end{aligned} \tag{29}$$

However, in order to approximate the cross derivatives we must allow for possible variation in both x and z terms so must consider the Taylor series in 2D as follows:

$$\begin{aligned} f(x + \mathrm{dx}, z + \mathrm{dz}) &= f(x, z) + \mathrm{dx}\frac{\partial f}{\partial x} + \mathrm{dz}\frac{\partial f}{\partial z}, \\ &+ \frac{1}{2}(\mathrm{dx}^2\frac{\partial^2 f}{\partial x^2} + 2\mathrm{dxdz}\frac{\partial^2 f}{\partial x \partial z} + \mathrm{dz}^2\frac{\partial^2 f}{\partial z^2}) + o(\mathrm{dx}^a\mathrm{dz}^b), \end{aligned} \tag{30}$$

where $a + b = 3$.
We will now generate the 2D Taylor series for each of the 4 combinations of +-dx and +-dz change from $f_{i,j}$:

$$\begin{aligned} f_{i+1,J+1} &= f_{i,j} + \mathrm{dx}\frac{\partial f}{\partial x}(x_i, z_j) + \mathrm{dz}\frac{\partial f}{\partial z}(x_i, z_j), \\ &+ \frac{1}{2}(\mathrm{dx}^2\frac{\partial^2 f}{\partial x^2}(x_i, z_j) + 2\mathrm{dxdz}\frac{\partial^2 f}{\partial x \partial z}(x_i, z_j) + \mathrm{dz}^2\frac{\partial^2 f}{\partial z^2}(x_i, z_j)) + o(\mathrm{dx}^a\mathrm{dz}^b), \end{aligned} \tag{31}$$

$$\begin{aligned} f_{i-1,J-1} &= f_{i,j} - \mathrm{dx}\frac{\partial f}{\partial x}(x_i, z_j) - \mathrm{dz}\frac{\partial f}{\partial z}(x_i, z_j), \\ &+ \frac{1}{2}(\mathrm{dx}^2\frac{\partial^2 f}{\partial x^2}(x_i, z_j) + 2\mathrm{dxdz}\frac{\partial^2 f}{\partial x \partial z}(x_i, z_j) + \mathrm{dz}^2\frac{\partial^2 f}{\partial z^2}(x_i, z_j)) + o(\mathrm{dx}^a\mathrm{dz}^b), \end{aligned} \tag{32}$$

$$\begin{aligned} f_{i-1,J+1} &= f_{i,j} - \mathrm{dx}\frac{\partial f}{\partial x}(x_i, z_j) + \mathrm{dz}\frac{\partial f}{\partial z}(x_i, z_j), \\ &+ \frac{1}{2}(\mathrm{dx}^2\frac{\partial^2 f}{\partial x^2}(x_i, z_j) - 2\mathrm{dxdz}\frac{\partial^2 f}{\partial x \partial z}(x_i, z_j) + \mathrm{dz}^2\frac{\partial^2 f}{\partial z^2}(x_i, z_j)) + o(\mathrm{dx}^a\mathrm{dz}^b), \end{aligned} \tag{33}$$

$$\begin{aligned} f_{i+1,J-1} &= f_{i,j} + \mathrm{dx}\frac{\partial f}{\partial x}(x_i, z_j) - \mathrm{dz}\frac{\partial f}{\partial z}(x_i, z_j), \\ &+ \frac{1}{2}(\mathrm{dx}^2\frac{\partial^2 f}{\partial x^2}(x_i, z_j) - 2\mathrm{dxdz}\frac{\partial^2 f}{\partial x \partial z}(x_i, z_j) + \mathrm{dz}^2\frac{\partial^2 f}{\partial z^2}(x_i, z_j)) + o(\mathrm{dx}^a\mathrm{dz}^b). \end{aligned} \tag{34}$$

Now we will employ the operation (31) + (32) - (33) - (34),

$$f_{i+1,j+1} + f_{i-1,j-1} - f_{i-1,j+1} - f_{i+1,j-1} = 4\mathrm{dxdz}\frac{\partial^2 f}{\partial x \partial z}(x_i, z_j) + o(\mathrm{dx}^a\mathrm{dz}^b).$$

However, because of opposing signs we need to check if we can refine the order of the remainder term to see if any cancellations occur. Using pascal triangle we can derive the coefficients of the terms. We can ignore the non-cross terms as they will always cancel under the operations

we apply. In addition the factorial outside the brackets will not help use determine if the term vanishes so can be ignored.

Equation	Additional Term
(31)	$3f_{xxz} + 3f_{xzz}$
(32)	$-3f_{xxz} - 3f_{xzz}$
(33)	$-3f_{xxz} + 3f_{xzz}$
(34)	$3f_{xxz} - 3f_{xzz}$
(31) + (32) - (33) - (34)	0

Table 1: Assuming $a + b = 3$

Equation	Additional Term
(31)	$4f_{xxxz} + 6f_{xxzz} + 4f_{xzzz}$
(32)	$4f_{xxxz} + 6f_{xxzz} + 4f_{xzzz}$
(33)	$-4f_{xxxz} + 6f_{xxzz} - 4f_{xzzz}$
(34)	$-4f_{xxxz} + 6f_{xxzz} - 4f_{xzzz}$
(31) + (32) - (33) - (34)	> 0

Table 2: Assuming $a + b = 4$

We can see that when a+b=3 the equations cancel, as a result once we divide through by 4dxdz we are left with the following equation:

$$\frac{\partial^2 f}{\partial x \partial z}(x_i, z_j) = \frac{f_{i+1,j+1} + f_{i-1,j-1} - f_{i-1,j+1} - f_{i+1,j-1}}{4\mathrm{dxdz}} + o(\mathrm{dx}^p \mathrm{dz}^q), \tag{35}$$

where p+q=2
5
Note by symmetry we also have:

$$\frac{\partial f}{\partial z}(x_i, z_j) \approx \frac{f_{i,j+1} - f_{i,j}}{\mathrm{dz}}, \tag{36}$$

$$\frac{\partial f}{\partial z}(x_i, z_j) \approx \frac{f_{i,j+1} - f_{i,j-1}}{2\mathrm{dz}}, \tag{37}$$

$$\frac{\partial^2 f}{\partial z^2}(x_i, z_j) \approx \frac{f_{i,j+1} + f_{i,j-1} - 2f_{i,j}}{\mathrm{dz}}. \tag{38}$$

Now we have discretised our differential equations we can fully describe the problem by imposing suitable boundary conditions. Our waves will only be allowed to propagate within the desired area.

6 Boundary Conditions

Stress T is force over area and in order to define suitable boundary conditions we must look at stress on the boundaries. A special case is a stress-free boundary or free surface, where a vacuum or material with low rigidity (e.g. the atmosphere) lies on one side of the boundary. In

this case, the traction on the surface is effectively zero, so the three stress components are zero. From [2] we know in general stress can be defined as:

$$T_{ij} = \lambda \sum_{k=1}^{3} \frac{\partial u_k}{\partial x_k} \delta_{ij} + \mu(\frac{\partial u_i}{\partial x_j} + \frac{u_j}{x_j}) = 0. \tag{39}$$

We can simplify this to our 2D model, recall that $u_2 = 0$, $\frac{\partial u_i}{\partial x_2} = 0$ and as such:

$$\begin{aligned} T_{13} &= \lambda \sum_{k=1}^{3} \frac{\partial u_k}{\partial x_k} \delta_{13} + \mu(\frac{\partial u_1}{\partial x_3} + \frac{\partial u_3}{\partial x_1}) = 0, \\ \delta_{13} &= 0 \quad \text{since } i \neq j, \\ 0 &= \mu(\frac{\partial v}{\partial z} + \frac{\partial w}{\partial x}), \end{aligned} \tag{40}$$

$$\begin{aligned} T_{33} &= \lambda \sum_{k=1}^{3} \frac{\partial u_k}{\partial x_k} \delta_{33} + \mu(\frac{\partial u_3}{\partial x_3} + \frac{\partial u_3}{\partial x_3}) = 0, \\ \delta_{33} &= 1 \quad \text{since } i = j, \\ T_{33} &= \lambda(\frac{\partial v}{\partial x} + \frac{\partial w}{\partial z}) + \mu(2\frac{\partial w}{\partial z}), \\ 0 &= \lambda \frac{\partial v}{\partial x} + (\lambda + 2\mu)\frac{\partial w}{\partial z}. \end{aligned} \tag{41}$$

Assuming dx = dz, the boundary conditions (40) and (41) can be expressed in discrete form becoming:

$$0 = v_{i,1} - v_{i,0} + \frac{1}{2}(w_{i+1,0} - w_{i-1,0}), \tag{42}$$

$$0 = \frac{\lambda}{2}(v_{i+1,0-v_{i-1,0}}) + (\lambda + 2\mu)(w_{i,1} - w_{i,0}). \tag{43}$$

To avoid unwanted reflection of the waves on the boundaries we add some absorption for the 3 sides of the domain by attenuating $\frac{\partial v}{\partial t}$ and $\frac{\partial w}{\partial t}$ on a strips of width l_d on the edges of figure the domain (2). We do this by damping the time derivatives after each integration steps,

$$\frac{dv_{i,j}}{dt} \rightarrow \frac{dv_{i,j}}{dt}(1 - \Gamma\frac{i}{N_d}) : \qquad i \in [0, N_d], j \in [0, N_z], \tag{44}$$

$$\frac{dv_{i,j}}{dt} \rightarrow \frac{dv_{i,j}}{dt}(1 - \Gamma\frac{N_x - i}{N_d}) : \quad i \in [N_x - N_d, N_x], j \in [0, N_z], \tag{45}$$

$$\frac{dv_{i,j}}{dt} \rightarrow \frac{dv_{i,j}}{dt}(1 - \Gamma\frac{N_z - j}{N_d}) : \quad i \in [0, N_x], j \in [N_z - N_d, N_z], \tag{46}$$

where Γ is a parameter which we usually take to be 0. Setting up suitable boundary conditions ensures the waves propagate as expected. However, the signal recorded will not be obvious so it can still be hard to interpret the result. We can help ourselves by displaying known paths alongside our wave equation's generated signal.

7 Ray Paths

We can use a simple ray model to predict the expected travel times of specific paths of successions of reflection and refraction. The idea is to assume waves behave like light such that they act as if they propagate along straight lines, but in all directions at once, we will then follow each individual ray one by one. In the homogeneous rock layers, the rays remain on a straight path, however when they hit the boundary between 2 layers, the rays are reflected and

refracted with the amplitude of each depending on the rock properties and the incident angle. Upon reaching a boundary waves will do some combination of reflect, refract or change wave type. So at each interface, each ray generates 4 new rays, as illustrated below in figure 7.

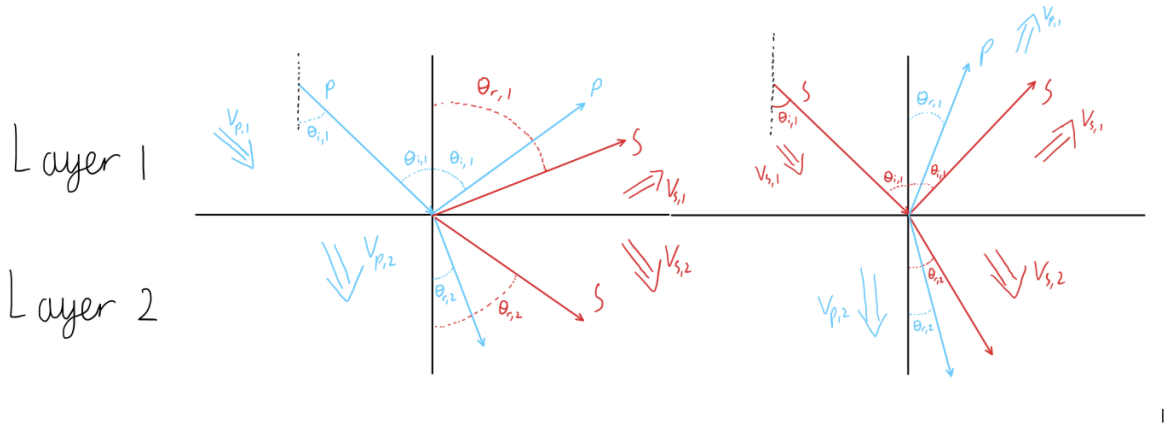

Figure 4: Simple Ray Model of Reflection and Refraction

In each layer, a ray will collide with a boundary at an incident angle ($0 < \theta < \frac{\pi}{2}$), the angle between the ray direction and the normal to layer interface (the vertical axis). Owing to the horizontal parallel nature of rock layers the incident angle at the top of the layer is the same as at the bottom of the same layer. The angles of refraction and reflection are then given by the Snell law:

$$\frac{\sin(\theta_1)}{\sin(\theta_2)} = \frac{V_1}{V_2}, \tag{47}$$

where V_1 is the speed of the incident wave and V_2 the speed of the refracted or reflected wave. Notice that when a wave reflected as a wave of the same type the speed $V_1 = V_2$ its incidence angle θ will remain unchanged. On the other hand this does not hold true if the wave is not reflected as a wave of the same type, in this case the incident angles will be different. It is important to note that there won't always be a solution to Snell's equation (47), this occurs when we get so called surface waves. In which case, we can take $\theta_2 = \frac{\pi}{2}$. In order to implement these ray path lines we must first generate general expressions to allow us to easily calculate the distance they cover and the time taken based on their original incidence angle.

7.1 Trajectories

As mentioned previously when we create our initial excitement as the waves propagate our 3 detectors will each receive signals of both v and w displacements. By producing a graph of these displacements against time we can observe a succession of blips representing the reflected and refracted waves, each following a different path. Each path, as shown in figure 5 and figure 6, will take a different length of time to travel back to the surface corresponding to a delayed blip on detector's signal. Our aim is to determine which path each of these blips corresponds to. We can consider specific paths through specific layers, mark and compare these results to the plots we obtain. This method will also allow us to determine the travel time of these waves and thus the travel time of our measured blips. We consider layers of thickness D_i, speed $V_{P,i}$ and $V_{S,i}$ where i is the layer index starting with i = 0 at the top. We consider a path $W_{0,i_0}, W_{1,i_1} W_{2,i_2}, ...W_{n,i_n}$ where W_{k,i_k} denotes the ray segment k of type W_k in layer i_k with incident angle θ_k. Q6

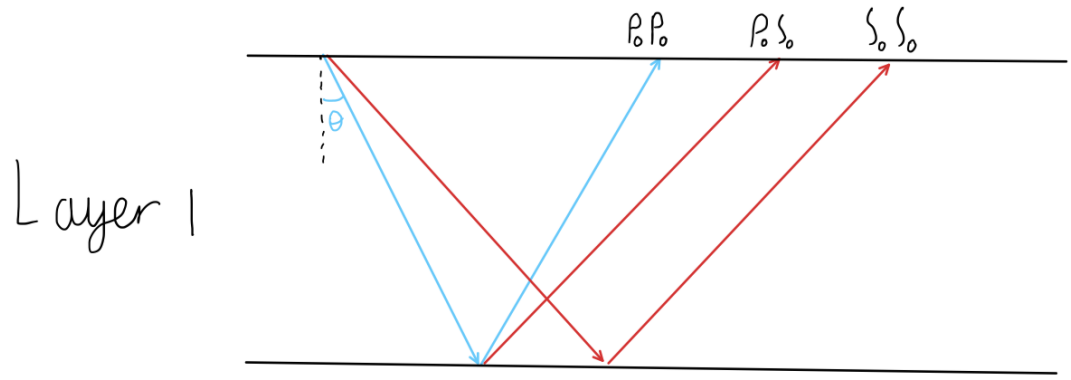

Figure 5: Some Ray Paths Within: 1 Layer

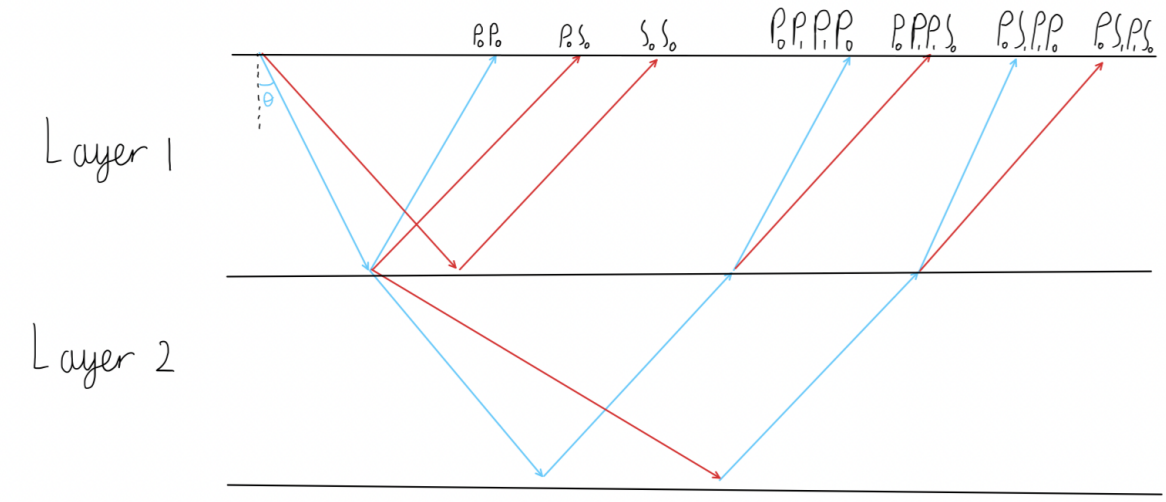

Figure 6: Some Ray Paths: 2 Layers

Firstly we will look at the horizontal covered by the ray if it goes through a layer of thickness D_i with an incidence angle θ_i till it reaches the next boundary,

$$\begin{aligned} \tan\theta_i &= \frac{x_i}{D_i}, \\ x_i &= D_i \tan\theta_i. \end{aligned} \tag{48}$$

Next we can look at the total distance covered by the ray inside the layer and the time it takes,

$$C_i = \frac{D_i}{\cos\theta_i}, \tag{49}$$

$$t_i = \frac{D_i}{V_{W_k,i}\cos\theta_i}. \tag{50}$$

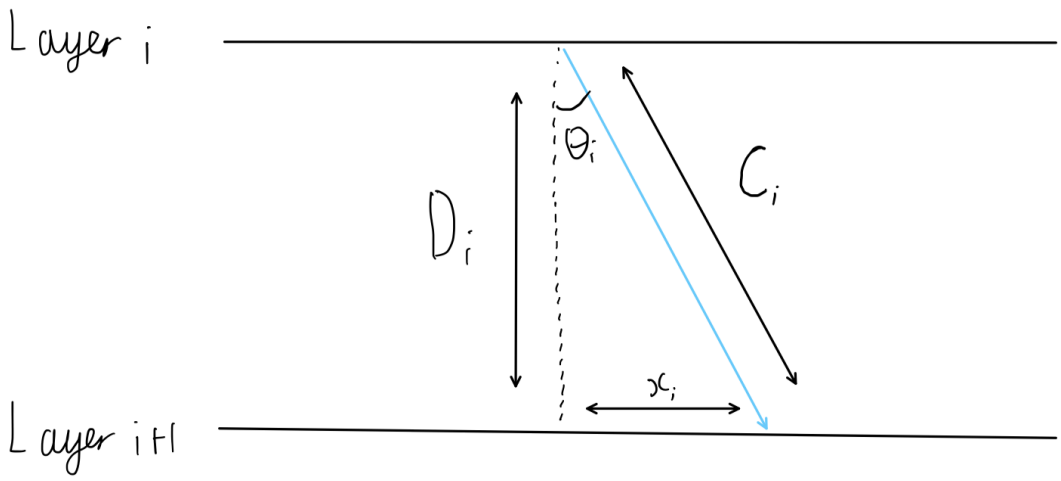

Figure 7: Ray Through Layer of Thickness D_i

Now in order to relate one layer to another we must derive a relationship between the theta from one layer to the next. Using Snell's Law (47),

$$\begin{aligned} \sin\theta_k &= \frac{V_{W_k,k}\sin\theta_{k-1}}{V_{W_k,k-1}}, \\ \theta_k &= \arcsin\left(\frac{V_{W_k,k}\sin\theta_{k-1}}{V_{W_{k-1},k-1}}\right). \end{aligned} \tag{51}$$

Using these results we can write an expression for the total time taken by the wave to cover the full path,

$$T = \sum_{k=0} \frac{D_k}{V_{W_k,k}\cos\theta_k}, \tag{52}$$

$$\theta_k = \arcsin\left(\frac{V_{W_k,k}\sin\theta_{k-1}}{V_{W_{k-1},k-1}}\right). \tag{53}$$

Using our equation for θ_k, we can determine a general equation for (53) in terms of θ_0,

$$\begin{aligned} \theta_1 &= \arcsin\left(\frac{V_{W_1,1}\sin\theta_0}{V_{W_0,0}}\right), \\ \theta_2 &= \arcsin\left(\frac{V_{W_2,2}\sin(\theta_1)}{V_{W_1,1}}\right), \\ &= \arcsin\left(\frac{V_{W_2,2}\sin[\arcsin(\frac{V_{W_1,1}\sin\theta_0}{V_{W_0,0}})]}{V_{W_1,1}}\right), \\ &= \arcsin\left(\frac{V_{W_2,2}\sin\theta_0}{V_{W_0,0}}\right), \\ \theta_3 &= \arcsin\left(\frac{V_{W_3,3}\sin\theta_2}{V_{W_2,2}}\right), \\ &= \arcsin\left(\frac{V_{W_3,3}\sin[\arcsin(\frac{V_{W_2,2}\sin\theta_0}{V_{W_0,0}})]}{V_{W_2,2}}\right), \\ &= \arcsin\left(\frac{V_{W_3,3}\sin\theta_0}{V_{W_0,0}}\right). \end{aligned}$$

This can then be generalised to the following:

$$\theta_k = \arcsin(\frac{V_{W_k,k}\sin\theta_0}{V_{W_0,0}}). \tag{54}$$

For instance we can look at an expression for the total time taken on the specific wave $P_0S_1P_1S_0$ in terms of θ_0 using equations (52) and (54),

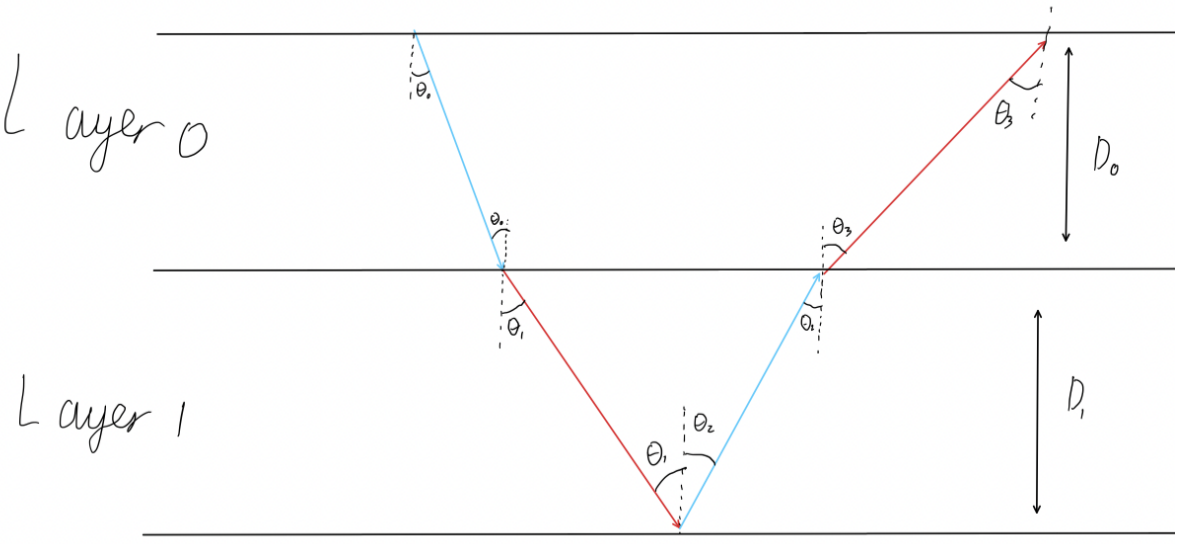

Figure 8: Ray Path of $P_0S_1P_1S_0$

$$\begin{aligned} T &= \frac{D_0}{V_{P,0}\cos\theta_0} + \frac{D_1}{V_{S,1}\cos\theta_1} + \frac{D_1}{V_{P,1}\cos\theta_2} + \frac{D_0}{V_{S,0}\cos\theta_3}, \\ &= D_0[\frac{1}{V_{P,0}\cos\theta_0} + \frac{1}{V_{S,0}\cos(\arcsin(\frac{V_{W_3,3}\sin\theta_0}{V_{W_0,0}}))}], \\ &+ D_1[\frac{1}{V_{S,1}\cos(\arcsin(\frac{V_{W_1,1}\sin\theta_0}{V_{W_0,0}}))} + \frac{1}{V_{P,1}\cos(\arcsin(\frac{V_{W_2,2}\sin\theta_0}{V_{W_0,0}}))}]. \end{aligned} \tag{55}$$

We have now considered how the specific path $P_0S_1P_1S_0$ will behave in general for a 2 layer model. This approach can be used to predict many other different paths of varying reflection complexity. Given the incident angle of the first segment of the ray, the Snell law allows us to determine the incident angle of the ray after each subsequent reflection or transmission and from this we can compute the horizontal offset in each layer. Summing over these gives the offset where the wave hits the surface again. What we need to do though is to consider the horizontal distance between the source and a detector and for each specific path determine the incident angle of the first segment so that the wave hits the detector after following that path. This can easily be done using the bisection method. Finally we will numerically simulate all of the components of our model together, everything from the discrete wave equations to the ray paths. After which conclusions may be drawn.

8 Numerical Simulations

8.1 Modelling Properties

To analyse the propagation of the seismic wave, we consider the 4km wide and 2km deep domain described above and we place the source at the surface in the middle of the domain,

$x = 2$km. The 3 detectors are then placed at $x = 2000$, $x = 2300$ and $x = 2500$. We consider 3 layers of rock made out of 500m of granite, 300m of shale and then 1200m of granite. The properties of the rocks are given in table 3 and the initial excitation is given by (17) [4], [5].

Rock	V_P (m/s)	V_S (m/s)	$\rho\ kg/m^3$
Granite	5980	3480	2660
Shale	2898	1290	2425

Table 3: Rock Properties Table

We can now use our assumed rock properties to calculate our Lamé parameters referenced earlier for granite. Simultaneously solving our equations (6) and (8) using our data in table 3,

$$\begin{aligned} V_S &= \sqrt{\frac{\mu}{\rho}}, \\ \mu &= V_S^2\rho, \\ &= 3480^2(2660), \\ &= 3.22 \times 10^{10} m^2 s^{-2} kg m^{-3}, \\ &= 32.2GPa. \end{aligned} \tag{56}$$

Using our value for μ we can now find λ,

$$\begin{aligned} V_P &= \sqrt{\frac{\lambda + 2\mu}{\rho}}, \\ \lambda &= V_P^2 \times \rho - 2\mu, \\ \lambda &= 30.7GPa. \end{aligned} \tag{57}$$

This λ (57) is consistent with [6]. The same process can be applied to find the Lamé parameters in the shale layer,

$$\begin{aligned} \mu &= 4.04GPa, \\ \lambda &= 20.4GPa. \end{aligned} \tag{58}$$

The simple ray paths we will implement to help interpret our results will be: P_0P_0, P_0S_0, S_0S_0, $P_0P_0P_0P_0$, $P_0P_1P_1P_0$, $S_0P_0P_0P_0$, $S_0P_1P_1P_0$ and $P_0S_0P_0S_0$. In order to differentiate effects and further understand the problem we will generate separate graphs for v, w and a final one for mod (the total displacement amplitude: $\sqrt{v^2 + w^2}$). Unlike geologists here we know the underground layers so there is no need for the sophisticated mathematical models used to extract the reflected waves they are interested in. Similarly though our measured signal contains the direct waves we are interested in as well as the noise. Here we will start by employing a simple model, this will be a 2km single layer of granite. Next we will then remove the displacement measured from our more complex model to hopefully remove some of the noise, we will call this the reduced signal.

8.2 Implementation

Q7

Using equation (17) we will generate our initial excitation. Initially this will start by propagating waves in the w direction not v, however this will change over time as the waves progress through the medium.

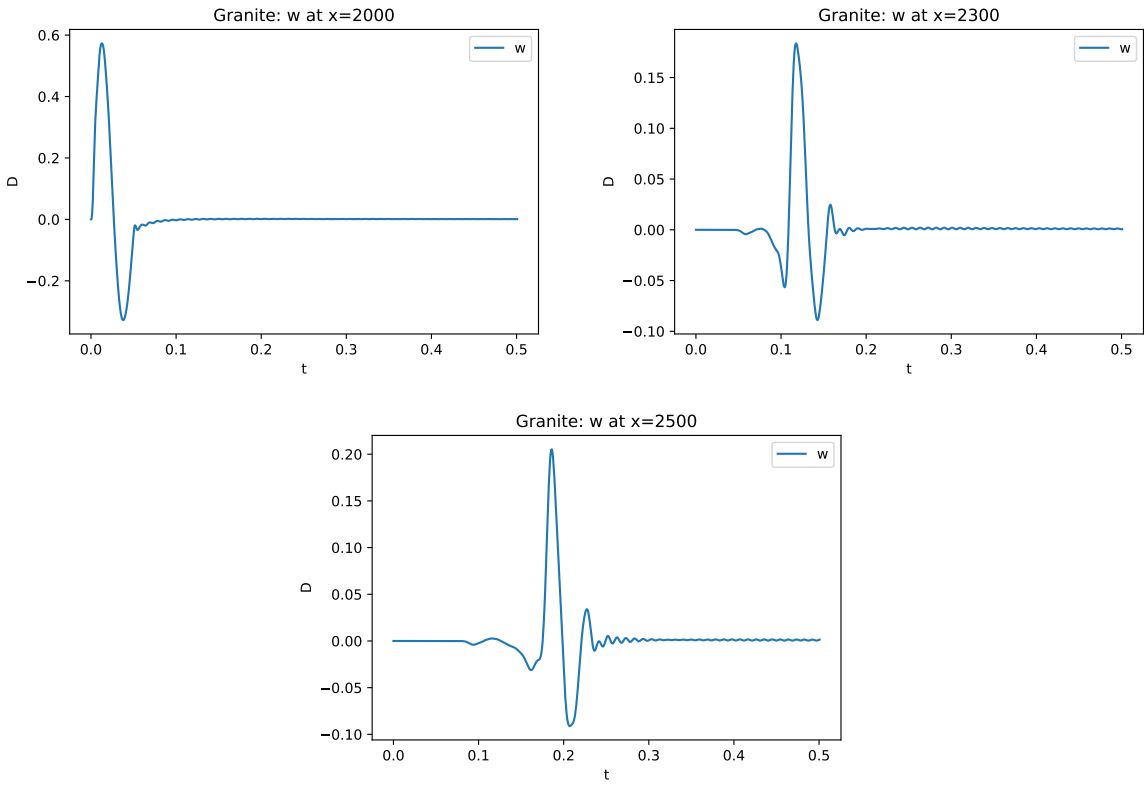

Figure 9: How w Waves Progress Through Time

Looking at figure 9 we can see how the initial w wave appears to propagate over time by looking at the displacement at each of our 3 detectors. The amplitude of the initial excitation also appears to decrease significantly from almost 0.6 to around 0.2. This may be due to some w waves transferring to become v waves or that the reflected waves will return to the detectors at times, the measured displacement will have more but flatter peaks. Moreover, by generating heat maps for different times we can differentiate between P and S waves. As can be seen in figure 10 the waves propagate through time and 2 wave fronts appear to form. The distance between these wave fronts increases with time suggesting they are each travelling at different speeds.

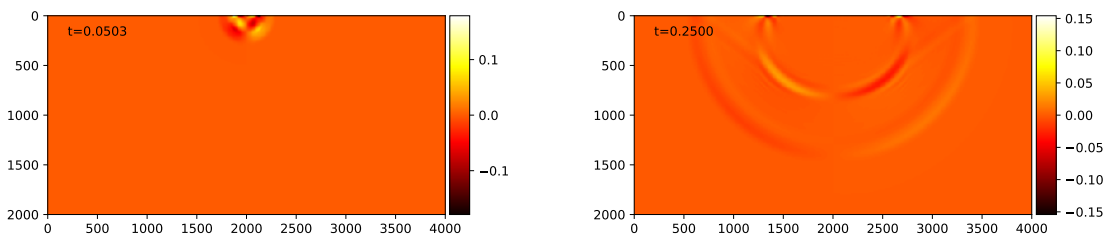

.5

Figure 10: Heat Maps for Single Granite Layer

In order to differentiate whether a P or S wave is faster we can refer to the speed values we have in table 3. P waves are faster in granite than S waves so we can conclude the outer wave front is a P wave and the inner is an S wave.
We will now move to using our more complex granite-shale-granite model. Observing the full signal measured on the detectors we can see from figure 11 our w propagates similarly to the simple granite only model.

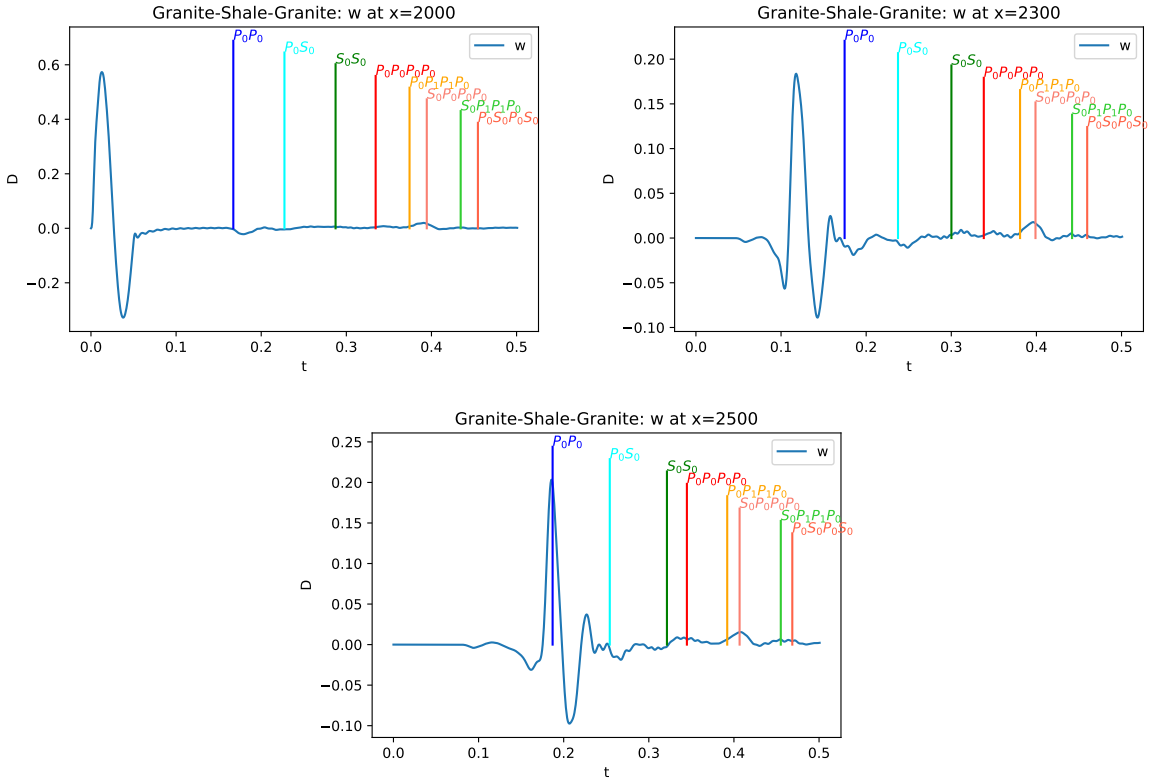

Figure 11: Granite-Shale-Granite w Wave Propagation

Now looking at v from figure 12 we can see that initially our v amplitude at x=2000 is numerically insignificant, this is because the initial wave generated is a w wave. As we look at the other detectors the reflected waves appear to come back at similar times to the w waves but of opposite displacement signs. Later reflected wave paths cannot be easily distinguished as there is too much noise from surface waves. Both figure 11 and figure 12 for w and v have some positive and negative blips of displacement. This comes from individual particles being forced to move in different directions relative to its starting position, as a result we define upwards movement relative to the initial position as positive but the opposite as negative.

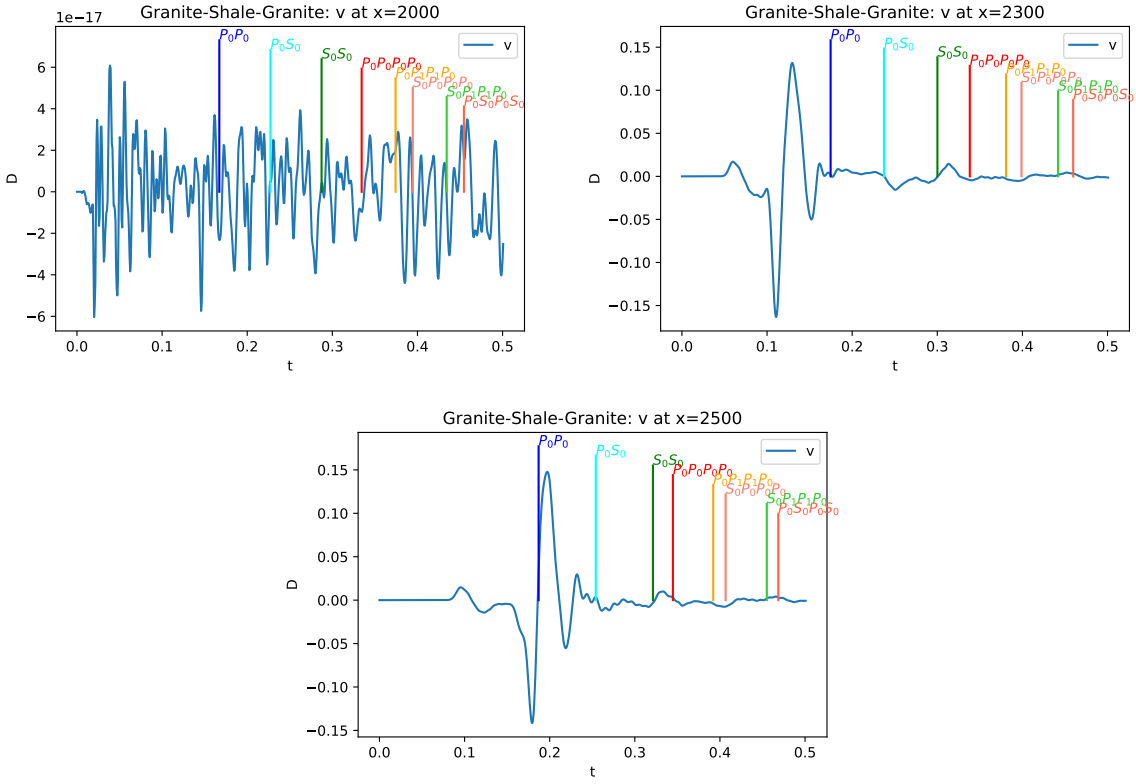

Figure 12: Granite-Shale-Granite v Wave Propagation

Now we will assess if subtracting the pure granite signal will help us draw better conclusions without the influence of surface wave noise. Here we will also employ the mod graphs in order to look at the effects of both waves on aggregate, removing the type of wave as a differentiating factor we need to account for.

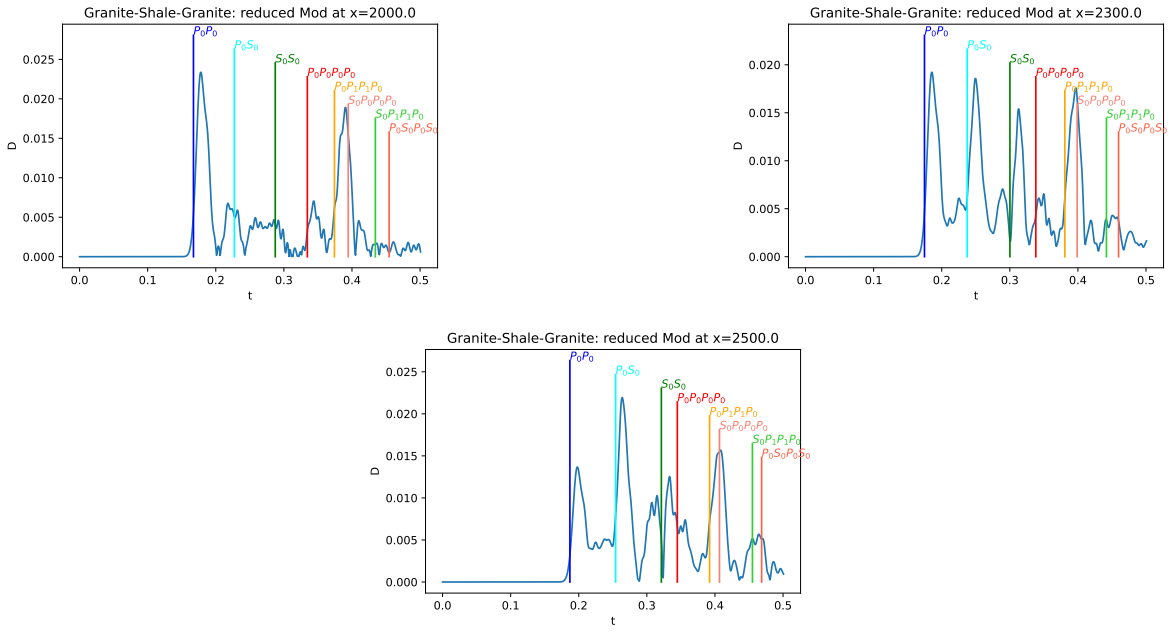

Figure 13: Granite-Shale-Granite Reduced Mod Propagation

Above in figure 13 we can see that by employing our subtraction method the initial wave appears to have entirely vanished. This is helpful in drawing conclusions as only the returning reflected waves appear as our measured displacement. The lack of noise this method produces also improves the effectiveness of our ray path approximation. This is because as the only peaks are the reflected rays the path lines line up much clearer. The ray path approximation is working well here as we can interpret the results of the simulation better. For all of the significant peaks of displacement it allows us to understand the travel path of the initial ray, whereas otherwise we would only be able to observe the final displacement of unknown ray paths. This in turn would help us gain the necessary information needed for more complex models such as final displacement, time taken and a rough path to infer about the underlying structure of the Earth.

9 Conclusion

Using our 2-dimensional seismic wave model we were able to predict how waves propagated from our initial brief excitation through our well defined domain. We saw that by using different detectors across the surface we could better trace waves from our initial excitation. In addition, we observed that by reducing our measured signal by a simple granite only domain the noise created by the surface waves was greatly reduced. Specific peaks of reflected waves could then be identified. Our simple ray path model then allowed us to identify the paths of these peaks and help calculate the time it takes them to propagate back to the surface. By using a method such as this the initial excitation wave equation could then be adjusted to test the impact of changes in the initial amplitude, frequency and medium have on the results. In addition, our model allows for easy application of other mediums instead of our granite-shale-granite domain. Together this information could then be used to make inferences about the underlying structure of the Earth's composition and to map subsurface structures among other uses.

References

[1] Seismic Wave, Wikipedia (2022) https://en.wikipedia.org/wiki/Seismic$wave$

[2] Nick Rawlinson Lecture notes on Seismology http://rses.anu.edu.au/nick/teaching.html

[3] Metal Earth Seismic Survey 2017, Harquail School of Earth Sciences https://www.youtube.com/watch?v=G$_nkMJxl - g$

[4] X. Zhang et al. Petrologic composition model of the upper crust in Bohai Bay basin, China, based on Lame impedances (2009) Applied Geophysics 6(4):327-336 DOI: http://doi.org/10.1007/s11770-009-0039-5

[5] Bill Goodway: AVO and Lam e Constants for Rock Parameterization and Fluid Detection https://csegrecorder.com/articles/view/avo-and-lame-constants-for-rock-parameterization-and-fluid-detection

[6] Lamé parameters of common rocks in the Earth's crust and upper mantle https://agupubs.onlinelibrary.wiley.com/doi/full/10.1029/2009JB007134